# Effect of the content of hydroxyapatite nano-particles on the properties and bioactivity of poly(L-lactide) - hybrid membranes

H. Deplaine, J.L. Gómez Ribelles, G. Gallego Ferrer


# Effect of the content of hydroxyapatite nano-particles on the properties and bioactivity of poly(L-lactide) – hybrid membranes

H. Deplaine, J.L. Gómez Ribelles, G. Gallego Ferrer

PII: S0266-3538(10)00235-6
DOI: 10.1016/j.compscitech.2010.06.009
Reference: CSTE 4744

To appear in: *Composites Science and Technology*

Received Date: 14 December 2009
Revised Date: 30 April 2010
Accepted Date: 20 June 2010

Please cite this article as: Deplaine, H., Ribelles, J.L.G., Ferrer, G.G., Effect of the content of hydroxyapatite nano-particles on the properties and bioactivity of poly(L-lactide) – hybrid membranes, *Composites Science and Technology* (2010), doi: 10.1016/j.compscitech.2010.06.009

# Effect of the content of hydroxyapatite nano-particles on the properties and bioactivity of poly(L-lactide) – hybrid membranes

H. Deplaine[1], J.L. Gómez Ribelles[1,2,3], G. Gallego Ferrer[1,2,3]

[1] *Centro de Biomateriales e Ingeniería Tisular, Universidad Politécnica de Valencia, PO Box 22012, E-46071 Valencia, Spain*

[2] *CIBER en Bioingeniería, Biomateriales y Nanomedicina, Valencia, Spain*

[3] *Centro de Investigación Príncipe Felipe, Autopista del Saler 16, E-46013 Valencia, Spain*

[*] Corresponding author. Address: Centro de Biomateriales e Ingeniería Tisular, Universidad Politécnica de Valencia, E-46071 Valencia, Spain. Tel: +34 96 387 7007, ext. 88929; Fax: +34 96 387 7276.

*E-mail address*: hardep1@upvnet.upv.es (Harmony Deplaine)

**Abstract**

Poly(L-lactide)/hydroxyapatite, PLLA, composite membranes for bone regeneration with different concentrations of nanoparticles have been prepared and their physicochemical properties and bioactivity have been determined. Hydroxyapatite nanoparticles act as nucleating agent of the poly(L-lactide) crystals, as detected by DSC, and as reinforcing filler, as proven by the monotonous increase of the elastic modulus of the microporous membranes with increasing nanofiller content. The bioactivity, which regards to the use of these materials in bone regeneration, was tested by immersing the samples in a simulated body fluid, SBF. A faster deposition of a biomimetic apatite layer was observed as increases the content of hydroxyapatite nanoparticles, thus membranes with a 15% (w/w %) of hydroxyapatite particles (relative to PLLA weight) present a homogeneous layer of hydroxyapatite on the surface of their pores after 7 days of immersion in SBF. An especial emphasis has been made on the influence of a plasma treatment on the bioactivity of the membranes. With this aim, the membranes were submitted to a plasma treatment previously to their immersion in a simulated body fluid. It has been observed that the surface of a PLLA membrane after 21 days of immersion in SBF is still not completely covered by hydroxyapatite whereas the same sample treated with plasma show a smooth layer of biomimetic hydroxyapatite. The increase of bioactivity achieved with this treatment was less important in high hydroxyapatite content composites.

***Keywords**: A.Poly(L-lactide), A.Hydroxyapatite, A.Nano composites, B.Bioactivity, B.Surface treatment.*

## 1. Introduction

Bone regeneration using tissue engineering techniques involve the use of bioresorbable scaffolds that should sustain the load applied "in vivo". Ceramic materials are brittle and stiff, and therefore macroporous materials made with them are fragile, while polymeric materials are unable to sustain the applied loads in many applications [1]. Nanocomposites formed by a polymeric matrix reinforced with hydroxyapatite (HA), other ceramic materials such as tricalciumphosphate, silica or bioactive glass have been proposed in order to design porous materials with adequate mechanical properties for bone engineering [2]. HA has the particularity to bind directly the bone without forming any surrounding connective tissue. HA has the same formulation of mineral bone ($Ca_{10}(PO_4)_6(OH)_2$). The rest of the resorbable ceramics are also based on calcium phosphate, but among them the quicker in degrading is HA [3]. Besides that, the presence of hydroxyapatite nanoparticles in the polymeric matrix can improve the bioactivity of the material, inducing osteogenesis when implanted "in vivo", due to osteoinductive and bone bonding ability [4]. This "in vivo" behaviour has been shown to be demonstrable by "in vitro" mineralization (Kokubo test). This experiment was proposed by Kokubo as an "in vitro" test to assess the bioactivity of a material by its capacity to generate a layer of HA on its surface when immersed in simulated body fluid (hereafter SBF) [5]. The mechanism proposed for this behaviour is that bioactive materials show negative surface potential when immersed in SBF, due to deprotonation at physiological pH of groups like –COOH, -OH, -TiOH (these groups have been shown to provoke hydroxyapatite precipitation in SBF) [6,7]. This negative charge attracts calcium ions, creating a Ca-rich layer with positive surface potential. This positive

surface recently formed, can in its turn attracts negative ions in solution like phosphate, leading to the deposition of a Ca-poor layer. This process repeats itself generating the HA layer on the surface of materials [8-10].

For this work poly(L-lactic acid), PLLA, was used, since it exhibits mechanical properties suitable for human bone applications. PLLA is a biocompatible and biodegradable polyester belonging to the group of poly α-hydroxy acids, and it can be easily processed into complex shapes. PLLA degrades by non-specific hydrolytic scission of its ester bonds thereby producing lactic acid which is a normal by-product of anaerobic metabolism in the human body [11-13]. In this work we present a series of PLLA/HA nano-composites membranes prepared by a freeze extraction process [14-16]. This method is based on phase separation, like liquid-liquid demixing, whereby the solvent and the polymer crystallises in the polymer-poor phase and the polymer-rich phase, respectively [17]; thus leaving a porous morphology when the crystallised solvent is removed with the aid of a good solvent. These membranes were then modified by plasma treatment in order to enhance their bioactivity [18]. As polymer containing carboxylic acids show high plasma susceptibility, the plasma treatment was applied as to help initiate the nucleation of a layer of HA. Oxygen plasma permits to lower the surface energy of PLLA, and consecuently increases the wettability as contact angle with water decreases after plasma exposure and the permeability of the membranes to SBF. Our AFM experiments allow concluding that the particles incorporated in the membranes do not show on the surface since they are covered by a thin layer of PLLA. This thin surface layer is directly attacked by the radicals and electrons of the plasma and thus HA particles show at the surface as observed in the SEM and AFM pictures. Apatite layer formation on the surface of the membranes was

observed after different times immersed in SBF as a means for studying "in vitro" bioactivity, the apatite layer density increases with the time of inmersion. The plasma treatment, by increasing the wettability of the membranes, as well as the increase of HA content in the composites, allows nucleating HA only after 7 days of immersion in SBF, what is not possible for pure PLLA. Moreover thermal and mechanical properties of the membranes were studied.

## 2. Materials and Methods

### *2.1. Materials*

PLLA from Purac biomaterials (The Netherlands) was used: it is a homopolymer of L-lactide with an inherent viscosity of 1.8 dl/g. The molecular weight distributions were analyzed by gel permeation chromatography using a Varian liquid chromatograph equipped with refractive index, UV, light scattering and viscosity detectors. Trichloromethane at 35 C was used as the eluent and the SEC columns were from Supelco (G6000-4000-2000 HXL). Thus, the optically pure PLLA has a number average molecular weight of 59,500 and a polydispersity index of 1.8. 1,4-dioxane was purchased from Scharlau Chemie, S.A.( Barcelona, Spain). Hydroxyapatite particles with particle size inferior to 200 nm were purchased from Sigma-Aldrich (Spain). The chemicals used in the preparation of SBF were from Sigma-Aldrich (Spain). All chemicals were used as received without any further purification.

### *2.2. Sample preparation*

A series of poly-L-lactic acid/hydroxyapatite composite membranes with HA content 0, 5, 10, and 15% (w/w) were prepared by freeze extraction method. Freeze extraction is a

modification of freeze drying process described by Ho et al [14]. The required quantity of HA powder was dispersed in dioxane by sonication, then a 15% weight PLLA (relative to solvent weight) was added to the mixtures, and stirred to complete dissolution. Four solutions with different content in HA were prepared, with 0, 5, 10, 15% particles by weight with regard to PLLA. The PLLA-HA solutions were poured into Teflon moulds and frozen in liquid nitrogen. Then, cold ethanol at -10ºC was poured on the frozen membranes in order to dissolve the crystallised dioxane. Dioxane extraction was conducted in a cold ethanol bath at -10ºC. Ethanol was replaced several times to ensure that most of the dioxane has been extracted from the samples, the PLLA is almost not plasticized and the pores do not collapse at room temperature. After extraction, membranes were dried in air atmosphere during 24h and then in vacuum to constant weight at room temperature. The membranes were cut into squares (1 cm x 1 cm) of 200 μm thickness. To obtain the desired thickness the samples were shaped included in resin O.C.T.$^{TM}$ compound from Tissue-Tek at -30ºC and cut by cryogenic microtome. After removing residues of O.C.T., samples were dried during three days. The first day at room temperature, the second under vacuum and the third under vacuum at 40ºC.

In order to analyze the effect of plasma treatment on the composites surface by AFM thin films were spin-casted from a 2% (2g/100ml) solution of PLLA in chloroform with a 10% (w/w) of HA (relative to PLLA weight) particles. Spin casting was performed on 12 mm glass coverslips at 2000 rpm for 30 s; previously to that process the mixture of the polymer solution and the particles was homogenised by sonication. Samples were dried in vacuo at room temperature before further characterisation.

*2.3. Bioactivity test*

SBF solution was prepared with the method of Müller *et al.* [19] from eight salt solutions of, KCl (59.64 g/l), NaCl (116.88 g/l), $NaHCO_3$ (45.37 g/l), $MgSO_4.7H_2O$ (49.30 g/l), $CaCl_2$ (14.702 g/l), TRIS (tris-hydroxymethyl aminomethane; 121.16 g/l) (used for pH adjustment, see below), $NaN_3$ (1 g/l), $KH_2PO_4$ (27.22 g/l) into 650 ml deionised ultra pure water, in order to prevent salt precipitation and maintain the pH of the solution. Then the solution was poured in a 1000 ml flask and filled with deionised ultra pure water. For pH adjustment to pH 7.6-7.7 at 25ºC (which corresponds to pH 7.3-7.4 at 37ºC), HCl or TRIS was added.

[Table 1.]

Samples were soaked in SBF for different times up to 21days. The SBF solution was not renewed during the first 7 days. Afterwards, the ion concentrations were adjusted to twice those of SBF (2xSBF) and the solution was renewed each 2-3 days, in order to provide more favourable conditions for apatite deposition. The samples treated with plasma were soaked in the SBF solution 1 hour after the treatment.

*2.4. Oxygen plasma treatment*

Surface modification was carried out with oxygen plasma (Plasma Electronic, model Piccolo, quartz cylinder, 2.45 GHz generator) at 300W in a 50 Pa vacuum, for 120 seconds for each side. Membranes were used for experiments immediately after exposure.

*2.5. Differential scanning calorimetry (DSC)*

Crystallinity was evaluated by thermal analysis with a Perkin Elmer DSC Pyris I. Two heating scans from 0ºC to 210ºC at 10ºC/min were performed, the first one in order to gain information on sample crystallinity after freeze extraction process, and the second

one in order to observe the behaviour of the samples after erasing thermal history and cooling down from 210ºC to 0ºC at 10ºC/min.

*2.6. Calcination experiments*

The real content of HA in the composites was determined by weighting membrane residues after calcination. Calcination was carried out in a Conatec HC-300 ceramic oven. For each concentration (0-5-10-15 wt.% HA), three samples were heated up to 600ºC at 10ºC/min, and maintained at 600ºC for 10 minutes, in order to entirely thermally degrade the PLLA.

*2.7. Dynamic mechanical spectroscopy (DMS)*

The dynamic mechanical analysis of the membranes before immersing in SBF was determined by the Seiko Instruments Extrar6000 Thermal Analysis and Rheology System. The samples were heated first from 0ºC up to 120ºC at 2ºC/min, maintained at 120ºC for 60 minutes, and then cooled to 0ºC at 2ºC and heated again to 150ºC. Testing frequency was 1 Hz, the membranes presented rectangular dimensions 3 x 3 x 30 $mm^3$.

*2.8. Hydroxyapatite morphology analysis and characterization*

For scanning electron microscope analysis, samples were mounted onto copper holders and gold sputtered. The morphology of the HA formed on the surface of the scaffold was characterized with a JEOL JSM 6300 scanning electron microscope in secondary mode under an acceleration tension of 15kV.

*2.9. Atomic force microscopy*

The effect of plasma treatment on the surface of the spin-casted films was observed by the amplitude images obtained with am Atomic Force Microscope, AFM, before and 24 hours after plasma treatment. *NanoScope III* from Digital Instruments operating in the

tapping mode in air and *NanoScope 4.43r8* software version was used. Si-cantilevers from Veeco (Manchester, UK) were used with force constant of 3 N/m and resonance frequency ranging from 66 and 94 kHz.

*2.10. Contact angle measurements*

A Dataphysics OCA instrument (DataPhysics Instruments GmbH, Filderstadt, Germany) and *SCA20* software were used to measure the contact angle on the surface of PLLA films of drops of water. Different drops of ultrapure water were deposited directly on PLLA films, before and after a plasma treatment (1 and 24 hours after). The volume used and the time between the drop deposition and the capture of the image were constant for each measurements (V = 0.20ml, t = 30s).

*2.11. Hydroxyapatite layer characterization*

Element quantification was performed by Energy Dispersive Spectroscopy, EDS, with a JEOL JSM 6300 scanning electron microscope with an acceleration tension of 10kV. For EDS analysis, samples were mounted onto copper holders and carbon sputtered. The samples were observed by SEM and EDS after 0, 7, 14 and 21 days in SBF with and without oxygen plasma treatment.

## 3. Results and discussion

*3.1. Membranes characterization*

The freeze extraction process produces a membrane with 10 μm micropores as shown in Figure 1. The micropores are homogenously dispersed on the surface of the membranes. To assure the reproducibility of the technique, 3 different membranes were fabricated

and observed by SEM. All membranes exhibited the same morphology. The pores are produced by the phase separation when both dioxane and PLLA crystallise from the solution. When producing a nano-composite membrane, the HA nano-particles are suspended in the solution. Crystallisation of PLLA entraps part of these particles but another part is expected to remain between different dioxane crystals or at the interfaces between dioxane and PLLA in the solid sample when immersed in liquid nitrogen.

[Fig.1. (left) and (right)]

The morphology of the membranes seems not to be affected by plasma treatment. After oxygen plasma treatment, as shown in Figure 2 some kind of abrasion defects can be seen on the surface of the membranes, which does not appear for the membranes without plasma treatment. Surface abrasion that was already found in plasma treated PLLA by Wang et al [18] can allow HA particles to appear at the pores walls.

[Fig. 2. (a) and (b)]

Although HA nano-particles cannot be seen by SEM, especially in the untreated membranes, probably because a layer of PLLA covers them, EDS analysis was able to show Ca and P peaks distinctive of the HA components as shown by the insets of Figures 2a and 2b. The EDS analysis was repeated three times in different zones for three different samples, and all the signals present the same behaviour, proving that particle dispersion is homogenous. AFM amplitude images (Figure 3) confirm these results. On one hand, as can be seen in Figure 3, the HA particles are uniformly dispersed in the PLLA matrix. Although the original particles are of sizes below 200 nm (as specified by Sigma Aldrich) it seems that some of them tend to agglomerate in the preparation process forming aggregates with sizes up to 300 nm. On another hand, AFM

pictures clearly show that there is a layer of PLLA covering the particles. The detail of an agglomerate of nanoparticles in Figure 3b is quite diffuse contrarily to what happens in the images took 24 hours after the plasma treatment, where the layer of PLLA covering the particles has been eliminated by plasma, and the particles are clearly exposed in the surface (Figure 3c). Even if there is a layer of PLLA covering the particles previously to the plasma treatment they can be detected by EDS because the beam electron trajectory of the EDS ray interacts with the material and can penetrate till 5 microns in the material [20].

[Fig. 3. (left) and (righ)]

*3.2. Calcination experiments*

[Table 2]

The calcination experiments showed that the amount of HA incorporated into the membranes is close but lower than the amount of HA dispersed in the PLLA solution. Membranes with 5, 10 wt.% HA (table 2) show 11-12% mass error, and 15 wt.% HA membrane mass error is 46%. These deviations can be an indication of an imperfect dispersion of particles, or the leaching of a part of the particles that remained in the solvent during phase separation.

*3.3. Differential scanning calorimetry (DSC)*

DSC experiments included a heating scan that gives information about the crystalline structure obtained after freeze extraction process. This scan was performed between 0

and 210ºC. Thus, at the end of this scan the sample is melted. A cooling scan followed to characterize the crystallization kinetics from the melting of the different nano-composites. Finally a second heating scan was recorded to characterize the structure of the polymer crystallized from the melt.

[Fig. 4. left and right.]

The first heating scan shows the glass transition with a large overshoot characteristic of the physical ageing (or structural relaxation) process suffered by the polymer during annealing at 40ºC while drying in vacuum. The cold crystallisation peaks appear after glass transition. These exothermal peaks appear at lower temperature as the HA nano-particles content increases (see Figure 4, left). Another crystallisation process appears at higher temperatures that is characteristic of highly nucleated samples that crystallize at very low temperatures [21,22], finally the melting process takes place at a temperature independent of sample composition. Cooling scan recorded after the first heating scan showed an exothermal peak (results not shown) that proves that PLLA partially crystallizes on cooling.

The second scan is representative of the samples crystallized after melting. Here the endothermal overshoot due to physical ageing disappears since the sample was not annealed below the glass transition (Figure 4, right). The crystallization and melting follow a trend similar to that of the first scan, although the crystallization peaks are clearly shifted towards higher temperatures. This behaviour can be explained by the formation of crystalline nuclei during physical ageing at temperatures below $T_g$ that has been proven in PLLA and in other semicrystalline polymers as well [23]. An increased number of nuclei at the beginning of cold crystallization speeds up the process; as a

result the observed crystallisation peak is sharper and shifted towards lower temperatures. The changes in shape and position for cold crystallisation peaks with increasing HA content demonstrate the nucleating effect of the HA nanoparticles [24].

The baseline used for the determination of crystallinity in the sample is presented as an example in Figure 4 in the thermogram corresponding to the second scan of the 15% HA composite. The determination of crystallinity was done by an integration of the heat flow trace with respect to it. This linear baseline joints a point immediately above the glass transition and another one after melting. If the sample was completely amorphous at the beginning of the heating scan the area between the thermogram and the baseline would be zero. The calculus becomes quite uncertain since the temperature interval to which it is extended is very broad and can easily lead to small errors in the determination of the baseline used in the integration (for instance for small curvatures in the baseline of the calorimeter). This difficulty is especially clear in the first scan when the thermogram starts deviating towards the exothermal side immediately above the glass transition (Figure 4, left), which impedes any enthalpy calculation. In the second scan crystallinity values between 6 and 20% were found but the HA content dependence was non-systematic. The crystallinity, $X$ (%), was determined based on the following equation:

$$X(\%) = \frac{\Delta H_m - \Delta H_c}{93.1} \cdot 100 ,$$

where $\Delta H_m$ and $\Delta H_c$ are respectively the melting and crystallization enthalpies, obtained from the integration of the heat flow thermograms, and the constant 93.1 J/g is the melting enthalpy for a 100% crystalline PLLA [23]. The onset of the glass transition seems to be independent to the filler content (Table 3). The difference between the

values measured in the first and second scan should be due to the physical ageing process to which samples were subjected during drying before the first scan. A slight decrease of the enthalpic glass transition temperature with the HA content is observed (Table 3).

[Table 3]

*3.4. Dynamic mechanical spectroscopy (DMS)*

Dynamic-mechanical experiments are also highly dependent on the thermal treatment to which the sample is subjected. The samples were first subjected to heating from 0 and 120ºC in the first measuring scan. The temperature dependence of the storage modulus, E' shows the sharp decrease starting close to the calorimetric glass transition. The shape of the curve with a change of slope in the middle of the relaxation indicates that crystallization starts during the scan itself, as seen in the DMTA curves (Figure 5a). This makes the values measured at temperatures above $T_g$ quite dependent on the thermal history in the scan itself. The modulus in the glass region measured in the first scan increases with the HA content of the composites (Table 1) showing the reinforcing role of the HA particles. To compare the behaviour of the different nano-composites with a more reproducible structure, samples were annealed at 120ºC for one hour to allow crystallization and cooled to 0ºC to start the second scan. Thus, the second scan corresponds to higher crystallinity samples. The main relaxation in the second scan is shifted to higher temperatures with respect to the first one. The value of E' in the glassy region increases with respect to the first scan due to the higher fraction of PLLA crystals. The reinforcing effect of the nanoparticles is clearly shown in the

semicrystalline samples both below and above the main relaxation of the amorphous phase (Figure 5b) [25].

[Fig. 5. (a) and (b)]

*3.5. Hydroxyapatite layer characterisation*

SEM analysis shows the influence on the kinetics of HA deposition during increasing immersion times in SBF. As noticed in Figure 6, PLLA is able to nucleate HA in its surface, without any special treatment but at very slow rates compared to plasma-treated PLLA or PLLA reinforced with HA. At short times a few nuclei can be observed in the SEM pictures, they increase in number to form a rough layer of cauliflower-shaped crystals [26]. The surface of the micropores appears uniformly coated by HA after an immersion time that decreases as the content of HA in the composite increases and with the plasma treatment. In order to show this behaviour with a reasonable number of Figures, Figure 6 shows the surface of a PLLA membrane after 21 days of immersion in SBF, a time at which coating is still not complete, whereas the sample treated with plasma show a smooth layer of biomimetic HA deposited on the surface. Although plasma treatment increases the bioactive potential of pure PLLA a faster process is needed to avoid degradation of the polymer before its osteo-integration. After 21 days in SBF or in the implantation site PLLA starts the degradation process and consequently its mechanical properties start to decrease too early making the material useless for bone tissue engineering. Consequently it is interesting to generate a layer of HA at shorter time of SBF inmersion (7 days in SBF) [27], an effect that has been obtained in this work by the addition of the HA particles.

[Fig. 6. left and right]

Figure 7 shows the effect of the HA nano-filler content after 7 days immersion. After this time the PLLA samples show no signs of apatite layer even when treated with plasma, but the rate of deposition increases with HA content and samples containing more than 10 wt.% HA nano-particles show a smooth coating of the composite surfaces. Plasma treatment further enhances the rate of deposition, and the thickness of the layer increases in such a way that biomimetic apatite fills the whole volume of the micropores (Figure 7). Results obtained after different immersion times in SBF (7, 14, 21 days) are similar. Figure 7 shows the typical cauliflower structure of the HA of the layer on the surface [28].

**Treated** **Untreated**

[Fig.7. (8 micrographs)]

[Table 4]

The water contact angle on PLLA before plasma treatment is 86.8º and it dramatically decreases to 22.6º one hour after plasma exposure. There is not too much difference between this value and that obtained 24 hours after plasma exposure, 25.1º, indicating that radicals recombination on the surface has been almost completed. The observed decrease indicates that the plasma treatment increases the wettability of the material, and so, the interaction between the ions in presence in SBF and the surface of the material. Consequently plasma treatment accelerates the process of precipitation of the ions on the surface of the material.

As can be seen on Table 4, Ca/P atomic ratio of the biomimetic HA layer has been calculated from EDS analysis. This ratio has been compared to the one of stoichiometric hydroxyapatite ($Ca_{10}(PO_4)_6(OH)_2$) Ca/P = 1.67, or physiological HA = 1.65. Globally

the Ca/P atomic ratio calculated for all the samples is higher than the physiological HA one, ranging from 1.63 to 2.54 (table 4) [28]. The membranes with HA incorporated at day 0, in which the Ca/P atomic ratio measured corresponds to the HA nanoparticles added as filler, have the highest ratio, and the ratio observed does not match that of stoichiometric hydroxyapatite claimed by the supplier. For the same immersion time membranes previously exposed to plasma present a ratio closer to the physiological one in comparison with membranes that had not been exposed to plasma. In general, the ratio that is closest to the physiological one is for the plasma treated membranes prepared with nano-filler after 7 days in SBF.

## 4. Conclusions

Freeze extraction allows obtaining PLLA/HA nano-composites with a good dispersion of HA particles and bioactive properties. The storage modulus increases with the filler content at temperatures above and below the glass transition of the amorphous phase. Particles act as a nucleating agent for PLLA modifying the crystallisation kinetics whereas glass transition temperature of PLLA is independent of the filler content. The bioactivity is enhanced by the presence of the HA particles more than by plasma treatment; indeed the nucleation of a biomimetic HA layer on the surface of the nano-composites when immersed in SBF is more effective than on PLLA membranes. This study allows combining two independent ways to increase the bioactivity of PLLA membranes: nanoparticles of HA content and plasma treatment. Our results show that membranes presenting the best interest for their use in bone regeneration are that with a 15% of HA nanoparticles and previously exposed to plasma. Indeed these membranes

present a good bioactivity, they are able to nucleate a layer of HA with a Ca/P ratio similar to the physiological one, after only 7 days in SBF, and so avoid a possible degradation of the material. Furthermore the content of HA is high and considerably reinforces the matrix. The composition of this membranes are a previous selection step to the design of scaffolds with suitable mechanical and morphological properties for their use in bone regeneration.

**Acknowledgements**

The authors acknowledge the support of the Spanish Ministery of Science and Innovation through the DPI2007-65601-C03-03 project (including the FEDER financial support). Dr. G. Gallego Ferrer acknowledges the support of the same Institution for the mobility grant JC2008-00135 in the "José Castillejo" program to do a research stay at the 3Bs Group from the Polymer Department of the University of Minho, Portugal. Furthermore the work of GGF and JLGR was partially supported by funds for research in the field of Regenerative Medicine through the collaboration agreement from the Conselleria de Sanidad (Generalitat Valenciana), and the Instituto de Salud Carlos III (Ministry of Science and Innovation).

**References**

[1] Gross K-A, Rodriguez-Lorenzo L-M. Biodegradable composite scaffolds with an interconnected spherical network for bone tissue engineering. Biomaterials 2004;25(20):4955–4962.

[2] Stevens MM. Biomaterials for bone tissue engineering. Mater Today 2008;11(5):18-25.

[3] Sastre R, de Aza S, Román J S. Biomateriales. In. Faenza editrice iberica s.l., editors. Faenza, Italiy

[4] Murphy WL, Hsiong S, Richardson TP, Simmons CA, Mooney DJ. Effects of a bone-like mineral film on phenotype of adult human mesenchymal stem cells in vitro. Biomaterials 2005;26(3):303-310.

[5] Kokubo T, Takadama H. How useful is SBF in predicting in vivo bone bioactivity? Biomaterials 2006;27(15)2907-2915.

[6] Oliveira AL, Mano JF, Reis RL. Nature-inspired calcium phosphate coatings: present status and novel advances in the science of mimicry. Curr Opin Solid St M 2003;7(4-5):309-318.

[7] Kawashita M, Nakao M, Minoda M, Kim HM, Beppu T, Miyamoto T. Apatite-forming ability of carboxyl group-containing polymer gels in a simulated body fluid. Biomaterials 2003;24(14):2477-2484.

[8] Landi E, Tampieri A, Celotti G, Langenati R, Sandri M, Sprio S. Nucleation of biomimetic apatite in synthetic body fluids: dense and porous scaffold development. Biomaterials 2005;26(16):2835-2845.

[9] Kim HM, Himeno T, Kokubo, Nakamura T. Process and kinetics of bonelike apatite formation on sintered hydroxyapatite in a simulated body fluid. Biomaterials 2005;26(21):4366-4373.

[10] Lu X, Leng Y. Theoretical analysis of calcium phosphate precipitation in simulated body fluid. Biomaterials 2005;26(10):1097-1108.

[11] Wong JY, Bronzino JD. Biomaterials. Biodegradable polymeric biomaterials: And updated overview. In: Wong JY, Bronzino JD, editors. Biomaterials. Boca Raton: Taylor and Francis Group, 2007.

[12] Wei G, Ma PX. Polymer/Ceramic composite scaffolds for bone tissue engineering. In: Peter X. Ma, Jennifer Elisseeff, editors. Scaffolding in tissue engineering, p. 241. Boca Raton: Taylor and Francis Group, 2006.

[13] Peibiao Z, Zhongkui H, Ting Y, Xuesi C, Xiabin J. In vivo mineralization and osteogenesis of nanocomposite scaffold of poly(lactide-co-glycolide) and hydroxyapatite surface-grafted with poly(L-lactide). Biomaterials 2009;30(1) 58-70.

[14] Ho MH, Kuo PY, Hsieh HJ, Hsien TY, Hou LT, Lai JY. Preparation of porous scaffolds by using freeze-extraction and freeze-gelation methods. Biomaterials 2004;25(1):129-138.

[15] Deville S, Saiz E, Tomsia A. Freeze casting of hydroxyapatite scaffolds for bone tissue engineering. Biomaterials 2006;27(32):5480-5489.

[16] Nejati E, Mirzadeh H, Zandi M. Synthesis and characterization of nano-hydroxyapatite rods/poly(L-lactide acid) composite scaffolds for bone tissue engineering. Compos Part A-Appl S 2008;39(10):1589-1596.

[17] Budyanto L, Goh YQ, Ooi CP. Fabrication and characterization of porous Poly (L-lactide) (PLLA) scaffolds using liquid-liquid phase separation. 4th International Conference on Biomedical Engineering, Kuala Lumpur, Malaysia: 2008. p.322-325.

[18] Qu X, Cui W, Yang F, Min C, Shen H, Bei J, Wang S. The effect of oxygen plasma pretreatment and incubation in modified simulated body fluids on the formation of bone-like apatite on poly(lactide-co-glycolide) (70/30). Biomaterials 2007;28(01):9-18.

[19] Müller L, Müller FA. Preparation of SBF with different $HCO_3^-$ content and its influence on the composition of biomimetic apatites. Acta Biomater 2006;2(2): 181-189.

[20] Goldstein JI, Newbury DE, Echlin P, Joy DC, Lyman CE, Lifshin E, Sawyer L, Michael JR. Scanning Electron Microscopy and X-ray Microanalysis. In: Kluwer Academic / Plenum Publishers, editors. New York, USA: 2003.

[21] Munehisa Y, Kazunari S, Yoshinori O, Wataru K. Melting behaviour of poly(L-lactic acid): X-ray and DSC analyses of the melting process. Polymer 2008;49 (7):1943-1951.

[22] Hernández Sánchez F, Molina Mateo J, Romero Colomer F, Salmerón Sánchez M, Gómez Ribelles JL, Mano JF. Influence of Low-Temperature Nucleation on the Crystallization Process of Poly(l-lactide). Biomacromolecules 2005;6(6),3291-3299.

[23] Lim LT, Auras R, Rubino M. Processing technologies for poly(lactic acid). Progr Polym Sci. 2008;33(8):820-852.

[24] Lebourg M, Suay Antón J, Gómez Ribelles JL. Porous membranes of PLLA-PCL blend for tissue engineering applications. Eur Polym. J 2008;44(7):2207-2218.

[25] Uskokovic PS, Tang CY, Tsui CP, Ignjatovic N, Uskokovic DP. Micromechanical properties of a hydroxyapatite/poly-L-lactide biocomposite using nanoindentation and modulus mapping. J Eur Ceram Soc 2007;27(2-3):1559-1564.

[26] Hong Z, Reis RL, Mano JF. Preparation and in vitro characterization of scaffolds of poly(L-lactic acid) containing bioactive glass ceramic nanoparticles. Acta Biomater 2008;4(5):1297-1306.

[27] Kang Y, Xu X, Yin G, Chen A, Liao L, Yao Y, Huang Z, Liao X. A comparative study of the *in vitro* degradation of poly(l-lactic acid)/β-tricalcium phosphate scaffold in static and dynamic simulated body fluid. Eur Polym J. 2007;43(5):1768-1778.

[28] Vallés Lluch A, Gallego Ferrer G, Monleón Pradas M. Biomimetic apatite coating on P(EMA-co-HEA)/$SiO_2$ hybrid nanocomposites. Polymer 2009; 50(13)2874-2884.

## Captions to Figures

**Fig. 1.** Scanning electron microphotographs of the surface of PLLA membranes before immersing in SBF: (left) low magnification micrograph and (right) high magnification micrograph.

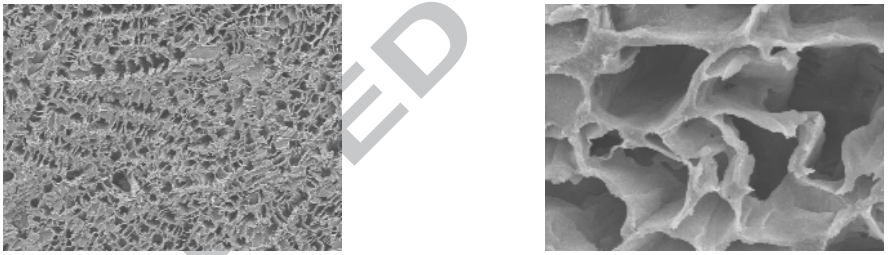

**Fig. 2.** Scanning electron micrographs and Energy dispersive spectroscopy analysis (as inset in the micrographs) of PLLA/HA nano-composites with 10 wt.% of HA, 0 days in SBF: (a) without plasma treatment, (b) with plasma treatment.

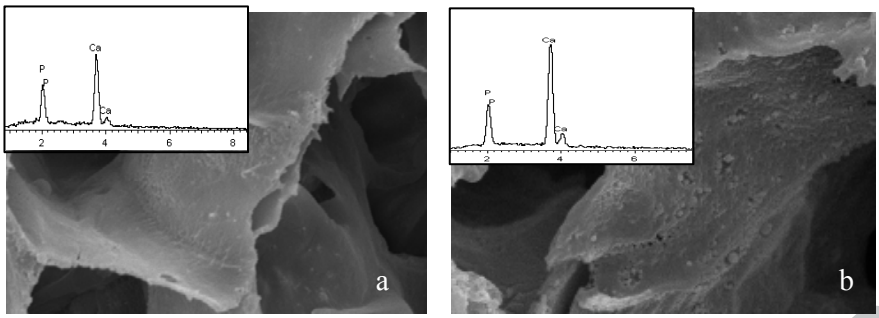


**Fig. 3**. Amplitude AFM images before plasma treatment (a) and 24 hours after plasma treatment (b and c).

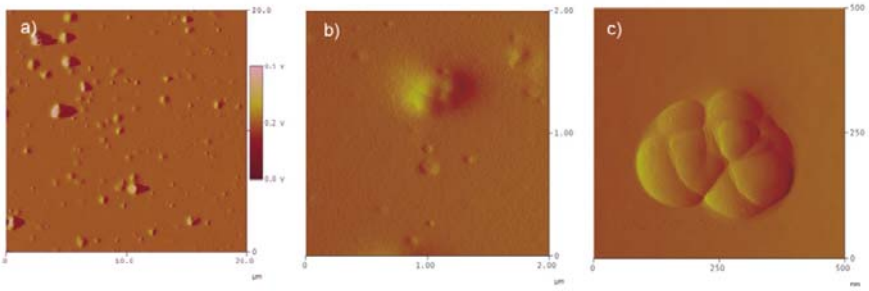


**Fig. 4.** First DSC heating scan of PLLA/HA nanocomposite with different filler content (left), and second DSC heating scan (right) obtained at a heating rate of 10ºC/min.

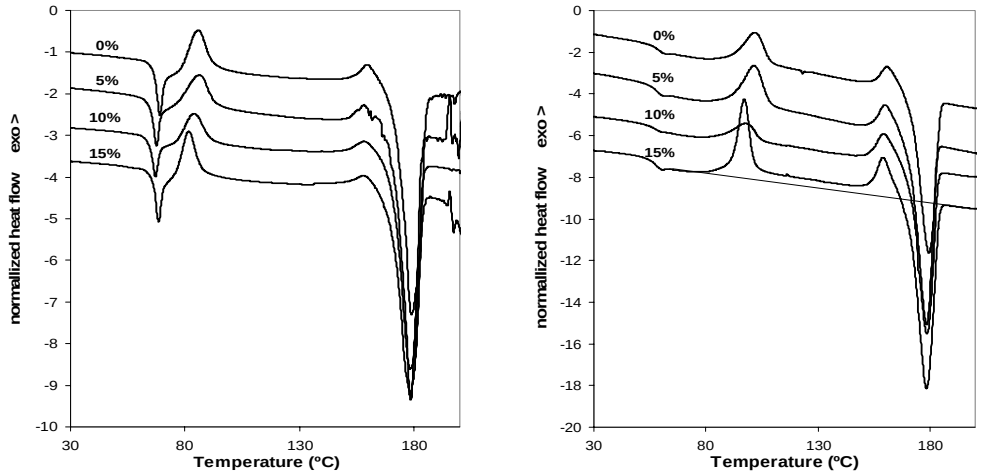

**Fig. 5.** Dynamic-mechanical storage modulus as a function of temperature, E'(T), obtained at 1Hz and a heating rate of 2ºC/min: (a) first and second heating scan of 10 wt.% HA membranes, (b) second heating scan of 0, 5, 10 and 15 wt.% HA membranes.

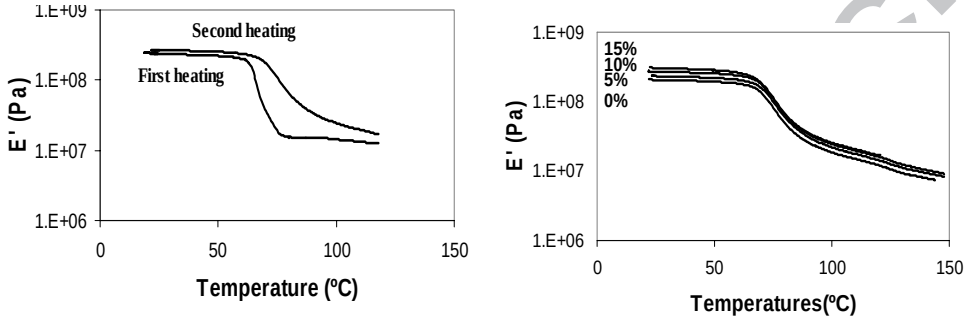


**Fig. 6.** Scanning electron micrographs of pure PLLA membranes, without plasma treatment (left) and with oxygen plasma treatment (right), after 21 days in SBF.

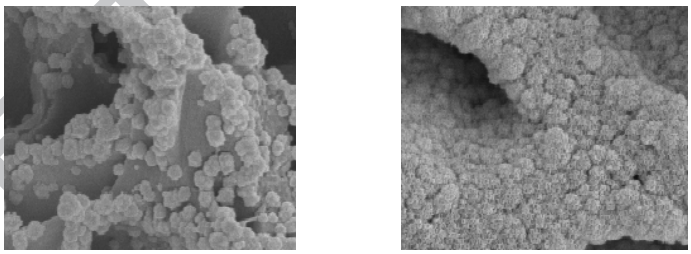

**Fig. 7.** Scanning electron micrographs of 0, 5, 10, 15 wt.% HA membranes without and with oxygen plasma treatment, after 7 days in SBF.

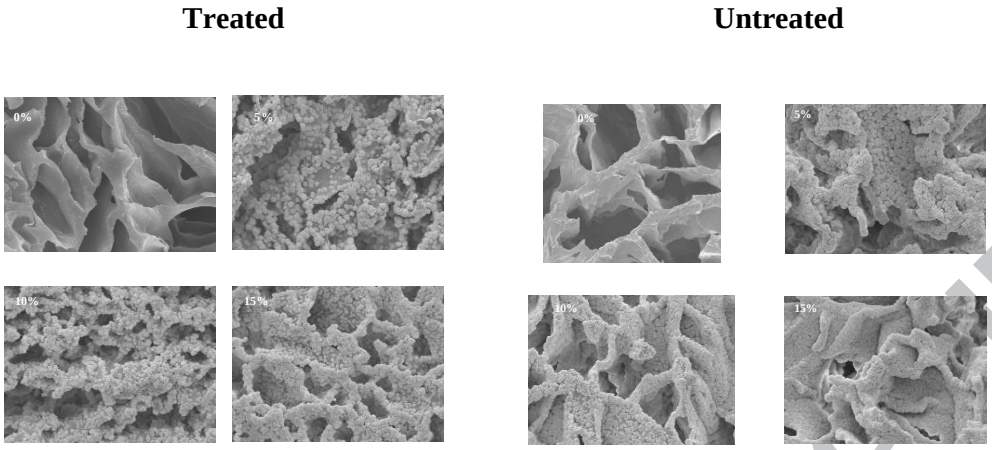


## Tables

### Table 1

Concentrated solutions volumes used for 1L of SBF

| Salts | KCl | NaCl | $NaHCO_3$ | $MgSO_4.7H_2O$ | CaCl | Tris.HCl | $NaN_3$ | $KH_2PO_4$ |
|---|---|---|---|---|---|---|---|---|
| volume (ml) | 5 | 60 | 10 | 5 | 25 | 50 | 10 | 5 |

### Table 2

Mass difference after and before calcinations

| HA content (%) | m (g) | m(g) | error (%) |
|---|---|---|---|
| | measured | theorical | |
| 0 | 0.002 ±0.006 | 0.000 | 0 |
| 5 | 0.042 ±0.004 | 0.048 ±0.005 | 11 |
| 10 | 0.074 ±0.006 | 0.084 ±0.007 | 12 |
| 15 | 0.073 ±0.010 | 0.092 ±0.008 | 46 |

### Table 3

Calorimetric glass transition temperatures and values of the dynamic-mechanical storage modulus in the glass, and after the main relaxation, for the first and second DMS heating scan, as a function of the HA content of the membranes.

| HA content (%) | Tg onset (ºC) | Enthalpic Tg onset (ºC) | E' glass | E' glass | E' (after main relaxation) | E' (after main relaxation) |
|---|---|---|---|---|---|---|
| | first scan | second scan | first scan | (30ºC) second scan | (30ºC) second scan | (120ºC) second scan |
| 0% | 51 | 36 | 62 | 1.81E+08 | 2.03E+08 | 1.20E+07 |
| 5% | 48 | 38 | 58 | 2.02E+08 | 2.30E+08 | 1.43E+07 |
| 10% | 51 | 38 | 58 | 2.37E+08 | 2.68E+08 | 1.60E+07 |
| 15% | 49 | 37 | 55 | 2.56E+08 | 3.03E+08 | 1.69E+07 |

**Table 4**

Ca/P atomic ratio reported from the Energy Dispersive Spectroscopy analysis

| Immersion time (days) | | 0 | | 7 | | 14 | | 21 | |
|---|---|---|---|---|---|---|---|---|---|
| HA content (%) | Plasma treatment | no | yes | no | yes | no | yes | no | yes |
| 0 | | 0 ±0 | 0±0 | 0±0 | 0±0 | - | - | 2.18 ±0.6 | 1.77 ±0.4 |
| 5 | | 2.54 ±0.5 | 2.15 ±0.4 | 1.82 ±0.1 | **1.66 ±0.1** | - | - | 2.55 ±0.7 | 1.77 ±0.3 |
| 10 | | 2.1 ±0.2 | 2.38 ±0.4 | 1.68 ±0.05 | **1.67 ±0.05** | 2.25 ±0.7 | 1.95 ±0.2 | 2.2 ±0.3 | 2.48 ±1.3 |
| 15 | | 2.21 ±0.3 | 2.33 ±0.4 | 1.63 ±0.1 | **1.69 ±0.2** | - | - | 2.08 ±0.2 | 2.62 ±1.4 |